Received: 15 September 2015 / Accepted: 17 December 2015 / Published online: 7 January 2016

Effects of Aluminium on Rat Brain Mitochondria Bioenergetics: an In vitro and In vivo Study

Javier Iglesias-González [1,3] • Sofía Sánchez-Iglesias [1] • Andrés Beiras-Iglesias [2] • Estefanía Méndez-Álvarez [1,4] • Ramón Soto-Otero [1,4]

* Ramón Soto-Otero ramon.soto@usc.es

1 Laboratory of Neurochemistry, Department of Biochemistry and Molecular Biology, Faculty of Medicine, University of Santiago de Compostela, Santiago de Compostela, Spain

2 Laboratory of Histology, Department of Morphological Sciences, Faculty of Medicine, University of Santiago de Compostela, Santiago de Compostela, Spain

3 Present address: The Healing Foundation Centre, Faculty of Life Sciences, University of Manchester, Oxford Road, Manchester M13 9PT, UK

4 Networking Research Center on Neurodegenerative Diseases (CIBERNED), Instituto de Salud Carlos III, Madrid, Spain

Abstract

Numerous studies have highlighted the potential of aluminium as an aetiological factor for some neurodegenerative disorders, particularly Alzheimer's disease and Parkinson's disease. Our previous studies have shown that aluminium can cause oxidative stress, reduce the activity of some antioxidant enzymes, and enhance the dopaminergic neurodegeneration induced by 6-hydroxydopamine in an experimental model of Parkinson's disease in rats. We now report a study on the effects caused by aluminium on mitochondrial bioenergetics following aluminium addition and after its chronic administration to rats. To develop our study, we used a high-resolution respirometry to test the mitochondrial respiratory capacities under the conditions of coupling, uncoupling, and non-coupling. Our study showed alterations in leakiness, a reduction in the maximum capacity of complex II-linked respiratory pathway, a decline in the respiration efficiency, and a decrease in the activities of complexes III and V in both models studied. The

observed effects also included both an alteration in mitochondrial transmembrane potential and a decrease in oxidative phosphorylation capacity when relatively high concentrations of aluminium were added to the isolated mitochondria. These findings contribute to explain both the ability of aluminium to generate oxidative stress and its suggested potential to act as an etiological factor by promoting the progression of neurodegenerative disorders such as Parkinson's disease.

Keywords
Aluminium. Mitochondria. High-resolution respirometry. Parkinson's disease. Oxidative stress. Rat brain

Abbreviations

Al^{3+}	Aluminium
ANT	Adenine nucleotide translocator
CI	Complex I
CII	Complex II
E	Uncoupled state

ETS	Electron transport system
ETSmax	Non-coupled respiration
FCCP	Carbonyl cyanide-4-(trifluoromethoxy)phenylhydrazone
L	Resting state after ATP synthase inhibition
mPTP	Mitochondrial permeability transition pore
OXPHOS	Oxidative phosphorylation
P	ADP activated state
PD	Parkinson’s disease
ROS	Reactive oxygen species
SOD	Superoxide dismutase
SUIT	Substrate-uncoupler-inhibitor-titration
TCA	Tricarboxylic acid cycle
TTP^+	Tetraphenylphosphonium
$\Delta\psi$	Mitochondria transmembrane potential

Introduction

Aluminium (Al^{3+}) is extensively used in daily life and in industrial processes providing a wide human exposition through air, tap water, food and some medications [1]. Although Al^{3+} has not been related with any biological function, a recent neurotoxicological study in humans has demonstrated that its accumulation into the aged brain constitutes a pathological risk [2]. Indeed, its presence at relatively high levels in the brain of some patients affected by Parkinson's disease (PD) has been reported [3, 4]. Aluminium has been also related with behavioural alterations [5], memory and learning deterioration [6], osteomalacia [7], dialysis encephalopathy [8], amyotrophic lateral sclerosis [9] and parkinsonism [10]. Although its role in Alzheimer's disease is not clear, it has been implicated in the development of neurofibrillar tangles [11, 12]. Also, the neurotoxicity of this metal has been often associated to its ability to promote the formation of reactive oxygen species (ROS) [13–15], a fact that is difficult to understand bearing in mind that Al^{3+} is a non-redox metal. Our previous work in an experimental model of PD in rats demonstrated that Al^{3+} crosses the blood brain barrier and it is accumulated into the rat brain [16]. Also, we highlighted its capacity to promote brain oxidative stress and to alter the activity of some antioxidant enzymes (i.e. catalase, superoxide dismutase and glutathione peroxidase) [17]. However, the precise molecular mechanism by which Al^{3+} reduces the activity of these antioxidant enzymes remains to be clarified. The development of new therapies in PD is strongly limited by the complexity of the neurodegenerative process itself, the lack of knowledge on the aetiological factors and its multifactorial character. Nowadays, the pharmacological treatments for PD have been designed to alleviate the symptoms of this disease and not to stop its development. Since metals have been considered as a pharmacological target in relation to neurodegenerative disorders, metal chelators have been proposed for the treatment of these disorders [18, 19] and, in particular, for the treatment of PD [20, 21].

Mitochondria play a central role as powerhouse of the cell, but are also involved in the regulation of the cell cycle, the redox signalling and as a main mechanism to trigger the apoptosis [22]. It is well-known that mitochondria are the major natural source of ROS due to the reported capacity of some complexes (I, II and III) of the electron transport system (ETS) to transfer electrons to oxygen molecules and form superoxide radical anions ($O^{\bullet -}$), which then are transformed to hydrogen peroxide (H_2O_2) by the superoxide dismutase (SOD)[2] [23]. Although it has been suggested that ROS produced by mitochondria may act as signalling molecules involved in the regulation of some cellular functions [24], it is also known that a mitochondrial dysfunction caused by a complex I defect may be an aetiological factor involved in the pathogenesis of PD [25, 26]. Indeed, the mitochondrial toxins that are often used to generate experimental models of PD commonly disrupt the ETS capacity and in this way promote oxidative stress [27, 28]. Consequently, the mitochondrial impairment and the foreseeable imbalance in the oxidative status of the cell are considered as the two main factors involved in the onset and development of PD [29]. Due to these

facts, the evaluation of mitochondrial bioenergetics represents a very valuable tool to understand the interaction between this organelle and a xenobiotic such as Al^{3+} in order to clarify the consequences for the cell. Previous studies have revealed that aluminium is capable to affect the activity of the ETS complexes [30] and increase ROS production [17, 30]. It has been also reported [31] the ability of Al^{3+} to bind the mitochondrial inner membrane andcause the opening of the membrane permeability transition pore (mPTP). Moreover, in a biological environment, the interaction between Al^{3+} and the superoxide radical anion is able to form the pro-oxidant aluminium superoxide semireduced radical ion and also to act as a catalyst of the irondriven oxidative stress (see [32] for a complete review). However, there are no studies analyzing the physiological respiration rates of the mitochondria in conditions of coupling, noncoupling and uncoupling in the presence of different substrates. Consequently, the aim of this study is to assess the effect of Al^{3+} on the bioenergetics of rat brain mitochondriaunder the described conditions, using high-resolution respirometry for the evaluation of mitochondrial respiratory capacities. In order to clarify possible differences depending on how the Al^{3+} is supplied, we performed a complete analysis using both an in vitro and in vivo experimental model.

Materials and Methods

Animals and Reagents

Male Sprague–Dawley rats (Experimental Animal Breeding Unit of the University of Santiago de Compostela, Santiago deCompostela, Spain) weighing 200–250 g were housed in ananimal room under controlled temperature (21 ± 1 °C) and a 12-h light–dark cycle (light on from 8 a.m. to 8 p.m.), with free access to tap water and standard laboratory chow. All experimental protocols were approved by the Ethical Committee of the University of Santiago de Compostela and conformed to the European Community Council Directive of November 24th, 1986 (86/609/EEC). Animals were allowed to acclimatize and exposed to an enriched environment for at least 4 days before the experiment [33]. To perform our in vitro experiments, a group of 12 rats was used during the study. For in vivo experimentation, a group of six rats was used as control and received a daily intraperitoneal (IP) saline solution (NaCl 0.9 %) for 10 days; a second group of six ratswas treated with a daily IP dose of aluminium chloride in saline (10 mg of Al^{3+}/kg/day) for 10 days. The IP injections were performed in the animal's lower left abdominal quadrant every morning at the same hour by a trained person according to an approved protocol by the Ethical Committee of the University of Santiago de Compostela. Injection solutions containing aluminium were prepared by dissolving aluminium chloride in saline, adjusting to pH 4.6 with sodium hydroxide and waiting the equilibration time necessary to obtain a clear solution [17]. The aluminium dosage regimen used was chosen to guarantee the accumulation of the metal in the rat brain [16]. Reagents were obtained from Sigma-Aldrich (St. Louis, MI, USA) unless otherwise stated.

Isolation of Rat Brain Mitochondria

Animals were under food deprivation overnight, stunned with carbon dioxide and sacrificed by decapitation. Forebrains of the two animals were dissected and pooled together into 30 ml of ice-cold isolation buffer (225 mM mannitol, 75 mM sucrose, 5 mM HEPES, 3 mM EDTA and 1 mg/ml fatty acid free BSA; pH 7.4). After homogenization, mitochondria were isolated by differential centrifugation as previously described [34]. This procedure yields 8–10 mg of protein per rat brain as was assessed by Bradford [35] with bovine serum albumin as standard. Mitochondria prepared following this protocol remain active for 3–4 h, as proved by the unchanging value obtained from flux control ratios. All the isolation procedure was carried out at 4 °C in order to maintain the temperature under control throughout the process.

Mitochondria Respiration

Respiratory assays were performed using high-resolution respirometry in a two-chamber respirometer at 37 °C (Oroboros Oxygraph-2k, Innsbruck, Austria) as previously described [34]. Briefly, mitochondria were fuelled with different substrates to analyze the respiration linked to complex I (10 mM glutamate, 2 mM malate and 5 mM pyruvate), complex II (after addition of 5 mM succinate and 0.1 mM rotenone) or complex I + II (10 mM succinate, 10 mM glutamate, 2 mM malate and 5 mM pyruvate). For in vitro experiments, and before the addition of substrates to avoid any interaction with the metal, mitochondria were pre-incubated with Al3+ for 3 min followed by centrifugation at 12,000×g for 10 min and reconstitution of the pellet in the respiration buffer to perform the bioenergetics assay. A substrate-uncoupler-inhibitortitration (SUIT) protocol was applied to obtain OXPHOS, LEAK and ETS respiratory rates for each sample. Sequentially, after the addition of the corresponding substrate to fuel the respiration, coupled respiration rate (OXPHOS) was monitored with the addition of saturating ADP (2.5 mM); uncoupled respiration under resting conditions (LEAK) was achieved with the addition of oligomycin (4 μg/ml; EtOH) and non-coupled respiration (ETSmax) was assessed using FCCP (0.5 μM). Flux control ratios were used in first term to determine the organelle integrity and functionality over time to avoid the evaluation of samples without optimal conditions.

Membrane Potential

Mitochondria were diluted to 0.3 mg/ml in 2.6 ml of a standard respiration medium and

assessed as described by Fasching and Gnaiger in 2009 [36]. The buffer was supplied with 1 mM of TPP^+ to evaluate the flux between the medium and the mitochondrial matrix during the experiments. Mitochondrial transmembrane potential ($\Delta\psi$) was estimated according to the transmembrane distribution of TPP^+ and expressed as arbitrary units to facilitate comparisons.

Measurement of Respiratory Chain Complexes Activities

The activities of complexes I, II, IV and V were measured in isolated mitochondria using the ELISA kits for rodents (Mitosciences®, Eugene, OR, USA), according to manufacturer's instructions. To perform the assays, mitochondria were isolated as described above and samples were processed adding 1/10 volume of detergent, incubated during 30 min and centrifuged for 20 min at 12,000×*g*. Subsequently, supernatants were collected and stored at −20 °C until their used.

For the assessment of complex III activity, the reduction of cytochrome c (15 μM) was monitored in the presence of coenzyme Q_{10} (100 μM) at 550 nm. To evaluate the chemical rate of reduction, cytochrome c and coenzyme Q_{10} were added to the assay medium containing 25 mM KH_2PO_4, 2 mM KCN, 5 mM $MgCl_2$ and 2 μg/ml rotenone at pH 7.2 and recorded for 3 min. Then mitochondria (0.25 mg/ml) were added and the increased in absorbance was measured for 5 min. Data are expressed as percentage of activity compared to control.

Electron Microscopy

Mitochondria were pre-incubated with Al^{3+} or in respiration buffer for 3 min followed by centrifugation at 13,000×*g* for 30 s, fixed by immersion for 45 min in 2.5 % glutaraldehyde in 0.15 M sodium cacodylate buffer (pH 7.3), postfixed with 2 % OsO_4 in the same buffer, dehydrated, embedded in Spurr's epoxy resin and sectioned. Sections were stained with uranyl acetate and lead citrate and examined in a Zeiss 902 electron microscope (Carl Zeiss, Oberkochen, Germany) at 80 kV accelerating voltage and film magnification of ×20, 000 or ×12,000.

Statistics

Statistical analyses were performed using Sigmaplot v. 11.0 (Systat Software Inc., Chicago,

IL, USA). The criteria of normality and homogeneity of variance for ANOVA were tested for each variable with Shapiro-Wilk and Spearman tests, respectively. If variances of different treatment groups were homogeneous, one-way ANOVA and, subsequently, Bonferroni paired comparisons as a post hoc test were applied to determine the level of significance between groups. Data are expressed as mean ± SE and the statistical significance for all tests was set at $p < 0.05$.

Results

Animal Response and Mitochondrial Structure

To analyze the general physiological effects of aluminium in the rats, both the weight and behaviour of the animals were controlled along the treatment. Average weight evolution on time of the animals treated in vivo is shown in Fig. 1a. In animals injected IP with Al^{3+}, a non-significant trend (10 mg/kg/day) in the body-weight gain is observed (Fig. 1a). However, these animals displayed no change in behaviour or in the whole-brain wet tissue weight when compared with control rats (data not shown).

Also, in order to evaluate the potential structural modifications derivative from the presence of aluminium, mitochondria were studied by electron microscopy as shown in Fig. 1b–g. Having into account that both cristae structure seem to depend on the bioenergetic status of the organelle [37] and the opening of mitochondrial permeability transition pore could promote swelling, we analyzed the micrographs from both models in active respiration state in the presence of substrates for complex I or complex I + II. The comparison of our in vitro and in vivo treatment showed no differences in the mitochondrial morphology caused by the presence of Al^{3+} when the respiration is fuelled with substrates linked to complex I (10 mM glutamate, 2 mM malate and 5 mM pyruvate; Fig. 1b–c). These organelles revealed a round or elongated shape with both a continuous membranous structure and internal cristae extensively folded. However, when Al^{3+} is present into the medium and the mitochondria are fueled with complex I + II substrate (10 mM glutamate, 2 mM malate, 5 mM pyruvate and 5 mM succinate), cristae shows a less dense matrix and tubular structure (Fig. 1f–g) in a clear opposition to the 'orthodox' conformation observed in the control micrograph (Fig. 1e). However, we would like to highlight that the external membrane still maintains the expected structure and that any of mitochondria showed a swelling phenotype (Fig. 1b–g).

Mitochondrial Bioenergetics

Bioenergetic studies were carried out using high-resolution respirometry in both models

studied (i.e. in vitro and in vivo) in order to analyze the ability of Al^{3+} to alter mitochondrial respiration. To select the concentration of Al^{3+} for in vitro assays, a preliminary study was performed exposing the organelles to a wide range of Al^{3+} concentrations. The study revealed a dose-dependent decrease in both OXPHOS and ETS_{max} capacities (Table 1). We found that 50 nM is an Al^{3+} concentration that significantly alters ($p < 0.001$) OXPHOS respiration, and in consequence, we decided to apply it to perform our in vitro assays as an acute treatment for the active respiratory state. Both experimental studies were carried out using a SUIT protocol that guarantee the analysis of the control exerted by different metabolic pathways (CI-, CII or CI + II-linked respiration) under the conditions of coupling, uncoupling and non-coupling. As shown in Fig. 2, in vitro OXPHOS respiration showed a significantly decrease for complex I (−81 %, $p < 0.001$) and complex I + II (−53 %, $p < 0.001$) respiratory capacities. Nevertheless, in vivo did not show significant alterations neither in complex I (−15 %) nor complex I + II (−18 %) OXPHOS capacities (Fig. 2). Moreover, the assessment of the non-coupled state linked to complex II revealed a decrease in the ETS_{max} activity (−42 and −44 %, $p < 0.001$) in the presence of Al^{3+} for both in vitro and in vivo, respectively. On the other hand, a decreased capacity for complex I + II ETS_{max} was found in vitro (−11 %, $p < 0.005$) but not in vivo (−7 %) (Fig. 2).

Flux control ratios were estimated to be used as coupling control ratios in order to understand both the metabolic control exerted by each respiratory pathway and the influence of Al^{3+} on it (Table 2). Under our experimental conditions, the control coupling ratio P/E expresses the limitation of OXPHOS capacity by the phosphorylation system (i.e. ANT, Pi translocator and ATP synthase). When P/E <1, the difference between OXPHOS and ETS_{max} capacities represents a wide mitochondrial respiratory capacity to modulate its response to energetic demands. However, when P/E = 0 state that the phosphorylation system does not exert any control on the respiration, consequently, it cannot be modulated in this way [38]. Our results for the P/E index (CI + IIP/CI + CIIE) showed a decreased in both models studied (i.e. −49 % in vitro and −14 % in vivo; $p < 0.001$; Table 2). In addition, the coupling control ratio L/E (CI + II_L/CI + CII_E) expresses both the leakiness and the efficiency of the mitochondrial coupling, allowing us to describe the existence of a dyscoupling effect due to a toxic action. In that sense, our data showed the existence of a differential effect depending on the experimental conditions used (Table 2), with an increase in the L/E index for in vitro experiments (47 %, $p < 0.001$) and a decrease for in vivo (−53 %, $p < 0.001$).

Aluminium Alters Complex III, Complex V and Proton Motive Force

The analysis of the proton motive force was assessed as a change in $\Delta\psi$ estimated using a TPP^+ electrode. Our results showed a differential effect of the metal over $\Delta\psi$, with a wide

decrease for in vitro experiments (−70 %, $p < 0.001$) and no effect for IP experiments (Fig. 3). Furthermore, the interaction of Al^{3+} with the enzymes of the ETS is one of the main reasons that could explain the decrease in respiration capacities. To evaluate this possibility, we assessed individually the enzyme activity of each complex in both models studied. Figure 4 shows altered activities for complex III (−23 %, $p < 0.001$) and complex V (−24 %, $p < 0.001$) for in vitro experiments. Moreover, when we supplied Al^{3+} in vivo, complex III activity decreased −17 % ($p < 0.01$) and complex V activity decreased −13 % ($p < 0.001$, Fig. 4). Finally, we also evaluated the complex IV respiratory capacity to work out if the Al^{3+} interaction with the ETS is up- or downstream Q-junction. Nevertheless, our data did not reveal a significantly inhibitory effect of Al^{3+} on complex IV activity (Fig. 4).

Discussion

The alteration of the mitochondrial homeostasis and the imbalance between free radical species production and the activity of the antioxidant systems have been highlighted as relevant factors involved in the development of neurodegenerative disorders and ageing [39]. Indeed, the oxidative stress production, the redox environment of the organelle and the redox signalling regulate mitochondrial function itself [40]. It is well-known that metals may play important roles on the redox environment due to both their catalytic capacity to promote ROS and their possible interaction with the clusters of the ETS. For this reason, the study of a metal such as Al^{3+} and its ability to alter mitochondrial respiration and redox environment gains importance for the development of new therapeutic strategies. In the present study, we demonstrate that Al^{3+} alters brain mitochondrial respiration. However, the extent and nature of this alteration seem to be differential depending on the conditions of metal exposition.

Mitochondria require a membranous system with a highly regulated permeability to generate the electrochemical potential that drives oxidative phosphorylation. During the in vitro acute exposition of mitochondria to Al^{3+}, our experiments revealed a significant leakiness of the mitochondria membrane as shown by both the dramatic increase in the L/E index and the dacay in $\Delta\psi$. Evidently, these facts suggest a dyscoupling of the organelle. A similar alteration promoted by Al^{3+} has been previously related with the opening of the mPTP [31] and the consequent uncoupling in the oxidative phosphorylation, both facts followed by impairment in cellular ATP production [41]. De Marchi et al. (2004) [42] also have attributed the opening of the mPTP to the ROS generated by Al^{3+} and its supposed ability to oxidise critical thiol groups in the poreforming structures of the membrane. In that last line, we have previously reported that a similar treatment with Al^{3+} causes brain oxidative stress and enhances the neurodegenerative damage induced by 6-hydroxydopamine in the rat nigrostriatal system [17]. However, our micrographs demonstrate that Al^{3+} is not able to promote swelling in the mitochondria that could be related with the mPTP

opening. We only have observed some alterations in the structure of the cristae that should be deeply analysed in future studies to determine if the fluidity of the membrane and its dynamics are compromised. Regarding to that, Van Rensburg et al. described in 1992 [43] a similar effect in an Alzheimer's disease model in which the fluidity of the membrane was modified by the presence of small amounts of Al^{3+}, and they attributed this observation to the binding of Al^{3+} to the phospholipids of the membrane. Controversially, our physiological exposition to Al^{3+} via chronic IP injection, on the one hand, did not show any alteration in the $\Delta\psi$ and, on the other hand, revealed a decrease in mitochondrial leakiness. We attribute these facts to the difference in the concentration of Al^{3+} present in each of both models and to the fact that the IP administration of Al^{3+} could favour the expression of natural chelants that can act protecting the cell (e.g. ferritin, transferrin, etc.).

As it is well-known, OXPHOS respiration requires the involvement of all mitochondria components (i.e. phosphorylation system, TCA, ETS and $\Delta\psi$) to achieve a coupled respiration. Our results appear to reveal that Al^{3+} alters OXPHOS respiration by acting at least in two different points of the ETS, one located upstream complex II and the other downstream. In downstream complex II, our results showed a significant decrease in OXPHOS capacity for in vitro exposition to Al^{3+} and only a decreasing trend for the in vivo IP treatment with Al^{3+}. In fact, the reduction on the enzymatic activity of complexes III and V due to the interaction with the metal explains our findings. We would like to highlight that the alterations in complex III has been also related with the production of ROS [44] and that could explain the oxidative stress that we previously reported [17]. A similar decrease in the enzyme activity for in vivo experiments has been also reported by other authors, showing alterations in all the ETS complexes activities, together with a decrease in the ATP turnover [30, 45]. Also, our P/E ratios for both in vitro and in vitro Al^{3+} exposition support the idea of an alteration in the phosphorylation system (i.e. ANT, P_i translocator and ATP synthase). Evidently, the control exerted by ATP synthase results essential to achieve a coupled respiration and the here reported decrease in the activity of this complex explains the respiratory deficiency. For this reason, our data demonstrated that Al^{3+} causes a loss of mitochondrial capacity to control the respiration through the phosphorylation system, a fact that could jeopardise the cell bioenergetics. On the other hand, the interaction of Al^{3+} upstream complex II is one of the main reasons that might explain the decrease of respiratory capacities in the ETS. From that point of view, our results showed that the presence of Al^{3+} in both models promotes a decrease on complex II-linked ETS_{max} capacity. However, the enzymatic activity of complex II was unaffected by the presence of Al^{3+}. Nevertheless, other previous studies reported an alteration in the activity of complex II in the presence of Al^{3+} together with an increase in ROS production [30, 46]. Assuming that Al^{3+} appears to cause inhibitory effects on biochemical reactions involving the binding to other metals such as Mg^{2+} and Ca^{2+} [47], a possible explanation to our here reported reduction in the complex II-linked ETS_{max} capacity could be an upstream inhibition of the aconitase activity or other enzymes of the TCA that use Ca^{2+}

as a cofactor, such as glutamate dehydrogenase [48].

In conclusion, Al^{3+} disrupts mitochondrial bioenergetics and promotes the dyscoupling of the organelle. Our data demonstrate that both in vitro and in vivo treatments alter the permeability and dynamic of the membranous systems, the ETS_{max} linked to the complex II and promote a decrease in the complexes III and V enzymatic activity. Indeed, the alteration of these parameters decreases the respiratory efficiency and the capacity of the mitochondria to modulate and control the energy production through the phosphorylation system. If we have in mind that the particular cellular architecture of the nigrostriatal dopaminergic neurons pushes the energetic capacity of the cell close to the edge [49], we could hypothesize that the lack of respiratory efficiency, the oxidative stress and the decrease in antioxidant enzymes activity [17] promote by Al^{3+} may contribute to the progression of neurodegenerative disorders as Parkinson's disease.

Acknowledgments

This study was financially supported by grant 09CSA005298PR from the Galician Government (XUGA), Santiago de Compostela, Spain.

References

1. Exley C (2013) Human exposure to aluminium. Environ Sci Processes Impacts 15:1807–18016
2. House E, Esiri M, Forster G, Ince PG, Exley C (2012) Aluminium, iron and copper in human brain tissues donated to the Medical Research Council's Cognitive Function and Ageing Study. Metallomics 4:56–65
3. Hirsch EC, Brandel JP, Galle P, Javoy-Aqid F, Aqid Y (1991) Iron and aluminium increase in the substantia nigra of patients with Parkinson's disease: a X-ray microanalysis. J Neurochem 56:446–451
4. Yasui M, Kihira T, Ota K (1992) Calcium, magnesium and aluminium concentrations in Parkinson's disease. Neurotoxicology 13: 593–600
5. Miu AC, Andreescu CE, Vaius R, Oltenau AI (2003) A behavioural and histological study of the effects of long-term exposure of adults rats to aluminium. Int J Neurosci 113:1197–1211
6. Julka D, Sandhir R, Gill KD (1995) Altered cholinergic metabolism in rat CNS following aluminium exposure: implications on learning performance. J Neurochem 65:2157–2164
7. Robertson JA, Felsenfeld AJ, Haygood CC, Wilson P, Clarke C, Llach F (1983) Animal model of alumium-induced osteomalacia: role of chronic renal failure. Kidney Int 23:327–335
8. Bolla KI, Briefel G, Spector D, Schwartz BS, Wieler L, Herron J, Gimenez L (1992)

Neurocognitive effects of aluminium. Arch Neurol 49:1021–1026
9. Perl DP, Gajdusek DC, Garruto RM, Yanagihara RT, Gibbs CJ (1982) Intraneuronal aluminium accumulation in amyotrophic lateral sclerosis and Parkinsonism-demaentia of Guam. Science 10:1053–1055
10. Garruto RM, Fukatsu R, Yanagihara R, Gajdusek DC, Hook G, Fiori CE (1984) Imaging of calcium and aluminium in neurofibrillary tangle-bearing neurons in parkinsonism-dementia of Guam. Proc Natl Acad Sci U S A 81:1875–1879
11. Zatta P, Lucchini R, Van Rensburg SJ, Taylor A (2003) The role of metals in neurodegenerative processes: aluminium, manganese and zinc. Brain Res Bull 62:15–28
12. Walton JR (2006) Aluminium in hippocampal neurons from humans with Alzheimer's disease. Neurotoxicology 27:385–394
13. Bondy SC, Ali SF, Guo-Ross S (1998) Aluminium but not iron treatment induces pro-oxidant events in the rat brain. Mol Chem Neuropathol 34:219–232
14. Kumar V, Gill KD (2009) Aluminium neurotoxicity: neurobehavioural and oxidative aspects. Arch Toxicol 83:965–978
15. Wu Z, Du Y, Xue H, Wu Y, Zhou B (2012) Aluminum induces neurodegeneration and its toxicity arises from increased iron accumulation and reactive oxygen species (ROS) production. Neurobiol Aging 33:199.e1–199.e12
16. Sánchez-Iglesias S, Soto-Otero R, Iglesias-González J, Barciela-Alonso MC, Bermejo-Barrera P, Méndez-Álvarez E (2007) Analysis of brain regional distribution of aluminium in rats via oral and intraperitoneal administration. J Trace Elem Med Biol 21:31–34
17. Sánchez-Iglesias S, Méndez-Álvarez E, Iglesias-González J, Muñoz-Patiño A, Sánchez-Sellero I, Labandeira-García JL, SotoOtero R (2009) Brain oxidative stress and selective behaviour of aluminium in specific areas of rat brain: potential effects in a 6OHDA-induced model of Prakinson's disease. J Neurochem 109:879–888
18. Gaeta A, Hider RC (2005) The crucial role of metal ions in neurodegeneration: the basis for a promising therapeutic strategy. Br J Pharmacol 146:1041–1059
19. Ward RJ, Dexter DT, Crichton RR (2012) Chelating agents for neurodegenerative diseases. Curr Med Chem 19:2760–2772
20. Levenson CW (2003) Iron and Parkinson's disease: chelators to rescue? Nutr Rev 61:311–313
21. Youdim MB, Stephenson G, Ben Sachar D (2004) Ironing iron out in Parkinson's disease and other neurodegenerative diseases with iron chelators: a lesson from 6-hydroxydopamine and iron chelators, desferal and VK-28. Ann NY Acad Sci 1012:306–325
22. Cadenas E (2004) Mitochondrial free radical production and cell signaling. Mol Asp Med 25:17–26
23. Kowaltowski AJ, de Souza-Pinto NC, Castilho RF, Vercesi AE (2009) Mitochondria and reactive oxygen species. Free Radic Biol Med 47:333–343
24. Chandel NS (2014) Mitochondria as signaling organelles. BMC Biol 12:34
25. Schapira AHV, Cooper JM, Dexter D, Jenner P, Clark JB, Mardsen CD (1989)

Mitochondrial complex I deficiency in Parkinson's disease. Lancet 1:1269
26. Keeney PM, Xie J, Capaldi RA, Bennett JP Jr (2006) Parkinson's disease brain mitochondrial complex I has oxidatively damaged subunits and is functionally impaired and misassembled. J Neurosci 26:5256–5264
27. Dauer W, Przedborski S (2003) Parkinson's disease: mechanisms and models. Neuron 39:889–909
28. Cannon JR, Greenamyre JT (2013) Gene-environment interactions in Parkinson's disease: specific evidence in humans and mammalian models. Neurobiol Dis 57:38–46
29. Schapira AHV (2008) Mitochondria in the aetiology and pathogenesis of Parkinson's disease. Lancet Neurol 7:97–109
30. Kumar V, Bal A, Gill KD (2008) Impairment of mitochondrial energy metabolism in different regions of rat brain following chronic exposure to aluminium. Brain Res 1232:94–103
31. Tonitello A, Clari G, Mancon M, Tognon G, Zatta P (2000) Aluminium as inducer of the mitocondrial permeability transition. J Biol Inorg Chem 5:612–623
32. Exley C (2004) The pro-oxidant activity of aluminium. Free Radic Biol Med 36:380–387
33. Schapiro SA, Everitt JI (2006) Preparation of animals for use in the laboratory: issues and challenges for the Institutional Animal Care and Use Committee (IACUC). ILAR J 47:370–375
34. Iglesias-Gonzalez J, Sánchez-Iglesias S, Beiras-Iglesias A, SotoOtero R, Méndez-Álvarez E (2013) A simple method for isolating rat brain mitochondria with high metabolic activity: Effects of EGTA and EDTA. J Neurosci Methods 213:39–42
35. Bradford MM (1976) A rapid and sensitive method for the quantitation of microgram quantities of protein utilizing the principle of protein-dye binding. Anal Biochem 72:248–254
36. Fasching M, Gnaiger E (2009) Determination of membrane potential with TPP+ and an ion selective electrode. Mitochondr Physiol Network 14(5):1–7
37. Manella CA (2006) Structure and dynamics of the mitochondrial inner membrane cristae. Biochim Biophys Acta 1763:542–548
38. Gnaiger E (2009) Capacity of oxidative phosphorylation in human skeletal muscle. New perspectives of mitochondrial physiology. Int J Biochem Cell Biol 41:1837–1845
39. Lin MT, Beal MF (2003) The oxidative damage theory of aging. Clin Neurosci Res 2:305–315
40. Daiber A (2010) Redox signalling (cross-talk) from and to mitochondria involves mitochondrial pores and reactive oxidative species. Biochim Biophys Acta 1797:897–906
41. Le Masters JJ, Nieminen A-L, Quian T, Lawrence C, Elmore SP, Nishimura Y, Crowe RA, Cascio WE et al (1998) The mitochondrial permeability transition in cell death: a common mechanism in necrosis, apoptosis and autophagy. Biochim Biophys Acta 1366:177–196
42. De Marchi U, Mancon M, Battaglia V, Ceccon S, Cardellini P, Tonitello A (2004)

Influence of reactive oxygen species production by monoamine oxidase activity on aluminium-induced mitochondrial permeability transition. Cell Mol Life Sci 61:2664–2671
43. Van Rensburg SJ, Carstens ME, Potocnik FCV, Aucamp AK, Taljaard JJF, Koch KR (1992) Membrane fluidity of platelets and erythrocytes in patients with Alzheimer's disease and the effect of small amounts of aluminium on platelet and erythrocytes membranes. Neurochem Res 17:825–829
44. Bleier L, Dröse S (2012) Superoxide generation by complex III: from mechanistic rationales to functional consequences. Biochim Biophys Acta 1827:1320–1331
45. Swegert CV, Dave KR, Katyare SS (1999) Effect of aluminiuminduced Alzheimer like condition on oxidative energy metabolism in rat liver, brain and heart mitochondria. Mech Aging Develop 112:27–42
46. Mailloux RJ, Hamel R, Appanna VD (2006) Aluminium toxicity elicits a dysfunctional TCA cycle and succinate accumulation in hepatocytes. J Biochem Mol Toxicol 20:198–208
47. Trapp GA (1980) Studies on aluminium interaction with enzymes and proteins-the inhibition of hexokinase. Neurotoxicology 1:89–100
48. Zatta P, Lain E, Cagnolini C (2000) Effects of aluminium on activity of Krebs cycle enzymes and glutamate dehydrogenase in rat brain homogenate. Eur J Biochem 267:3049–3055
49. Bolam JP, Pissadaki EK (2012) Living on the edge with too many mouths to feed: why dopamine neurons die. Mov Disord 27:1478–1483

Fig. 1

a Effect of aluminium exposure on body weight gain (control, *filled circle*; Al^{3+} treated with a daily IP dose of 10 mg Al^{3+}/kg/day for 10 days, *open circle*). b–g Mitochondrial structure observed by electron micrograph in both control and after exposition to Al^{3+}. The fixation of the organelles was performed during OXPHOS respiration fuelled by substrates linked to CI (b–d) or CI + II (e–g). b Control group; c Al^{3+} 50 nM added in vitro (50 nM); d Al^{3+} treated with a daily IP dose of 10 mg Al^{3+}/kg/day for 10 days; e control group; f Al^{3+} added in vitro (50 nM); g Al^{3+} treated with a daily IP dose of 10 mg Al^{3+}/kg/day for 10 days

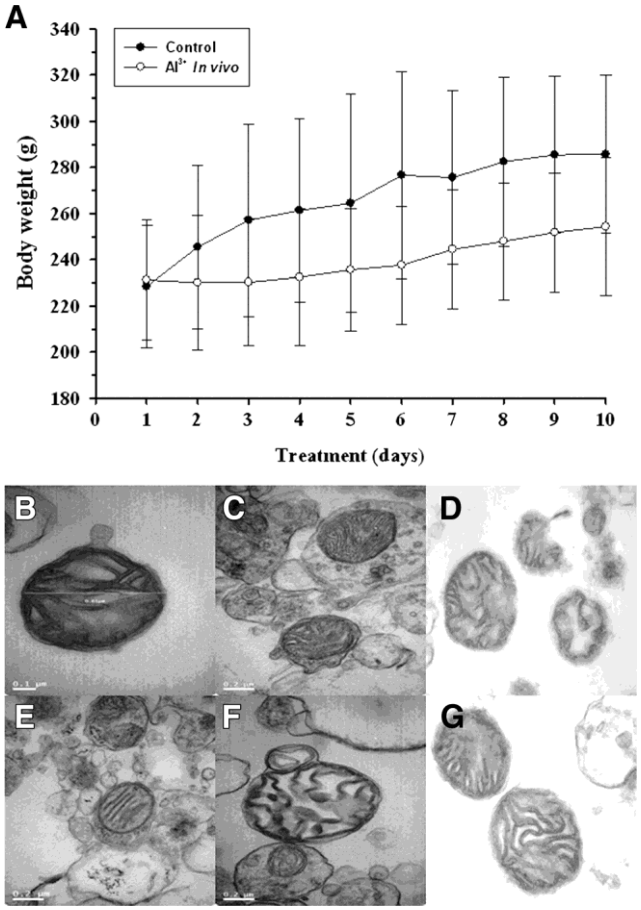

Fig. 2

Effects of Al^{3+} on mitochondrial respiratory capacities for in vitro experiments (50 nM Al^{3+}) and in vivo experimentation (daily IP dose of 10 mg Al^{3+}/kg/day for 10 days). Mitochondrial coupling states are differentiated as OXPHOS (saturating ADP, 1.5 mM) and ETS_{max} (noncoupled). Data are means ± SE; $n = 6$. *Significant difference (at least $p < 0.05$) tested by one-way ANOVA and Bonferroni post hoc

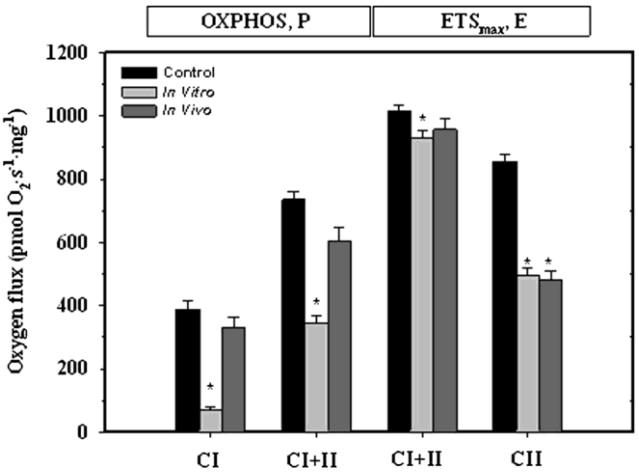

Fig. 3

Effects of Al^{3+} on membrane potential for both in vitro experiments (50 nM Al^{3+}) and in vivo experimentation (daily IP dose of 10 mg Al^{3+}/kg/day for 10 days). Data are means ± SE; $n = 6$. *Significant difference (at least $p < 0.05$) when compared with control (one-way ANOVA and a Bonferroni post hoc)

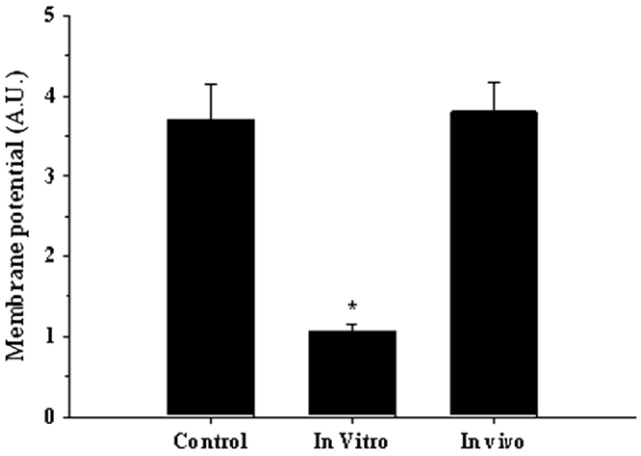

Fig. 4

Effects of Al^{3+} on enzymatic activity of each of the electron transport system complexes for both in vitro experiments (*black*; 50 nM Al^{3+}) and in vivo experimentation (*grey*; daily IP dose of 10 mg Al^{3+}/kg/day for 10 days). Data are means ± SE; $n = 6$. *Significant difference (at least $p < 0.05$) when compared with control (one-way ANOVA and a Bonferroni post hoc)

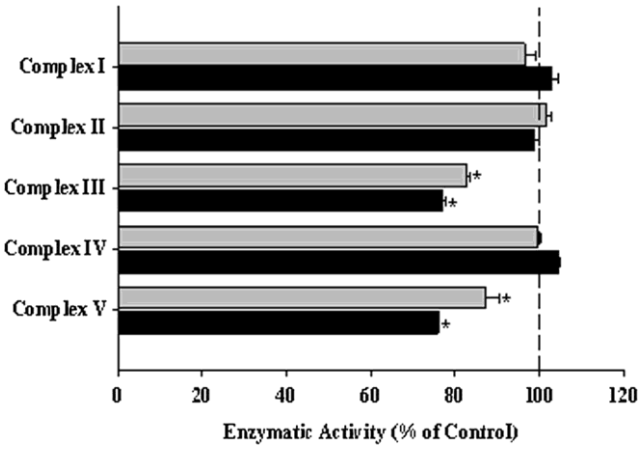

Table 1

Respiratory parameters obtained when a SUIT protocol was applied to isolated rat brain mitochondria after a pre-incubation with different concentrations of Al^{3+} for 3 min (see Material and Methods for details): OXPHOS and ETS_{max} capacities.

Group	OXPHOS (pmol O_2 s^{-1} mg^{-1}) CI: GM_P	ETS_{max} (pmol O_2 s^{-1} mg^{-1}) CI: GM_E
Control	388.66 ± 19.27	717.45 ± 10.98
5 nM	203.41 ± 19.36*	375.69 ± 2.30*
10 nM	137.45 ± 10.45*	306.93 ± 16.88*
50 nM	72.43 ± 7.34*	247.98 ± 17.28*
100 nM	21.94 ± 1.48*	238.41 ± 29.13*
1 μM	25.55 ± 2.93*	78.79 ± 13.55*
10 μM	28.76 ± 3.05*	87.30 ± 12.65*
100 μM	23.23 ± 0.97*	20.08 ± 2.64*

Data are means ± SE; $n = 6$. *Significant difference (at least $p < 0.05$) tested by one-way ANOVA and Bonferroni post hoc

Table 2

Effects of Al^{3+} on flux control ratio (FCR) obtained for each model studied using CI + II_E capacity to normalize. Data are means ± SE; n =6

Group	FCR	
	$CI + CII_P/CI + CII_E$ (P/E)	$CI + CII_L/CI + CII_E$ (L/E)
Control	0.722 ± 0.005	0.061 ± 0.005
In vitro	0.372 ± 0.002*	0.149 ± 0.001*
IP treatment	0.628 ± 0.004*	0.029 ± 0.001*

*Significant difference (at least $p < 0.05$) tested by one-way ANOVA and Bonferroni post hoc